AWES2020
20th Australasian Wind Engineering Society Workshop
8 – 9 April, 2021

Wind tunnel experiments of air pollutant residual time around a generic building

Erfan Keshavarzian[1], Kenny Kwok[2], Kejun Dong[1], Kapil Chauhan[2], Yu Zhang[3]
[1]*Centre for Infrastructure Engineering, School of Engineering, Western Sydney University, NSW 2751, Australia.*
[2]*School of Civil Engineering, The University of Sydney, NSW 2006, Australia.*
[3]*School of Medicine, Tsinghua University, Beijing 10 0 048, China.*

ABSTRACT

This paper presents an experimental study of air pollutant residual time in haze-fog (HF) phenomenon around a generic isolated building. A complex set-up is designed to simulate pre-mixed stagnant tracer gas as HF. Normalized air pollutant residual time is analyzed for the windward and leeward regions near the building model. The experimental data confirm that the residual time is dominated by wind-structure interaction and is consistent with wind characteristics around the building model. The air pollutant residual time for the full-scale model is estimated based on the scaled model tested in the wind tunnel. The results provide new insights into the air pollutant residual times and can be used to validate Computational Fluid Dynamics (CFD) simulations of the same.

1. Introduction

Densely populated urban areas are more challenging to optimize the design for the benefits of natural ventilation. Apart from higher air pollutant emissions related to human activities in these urban areas, stagnant or slow airflow due to closely packed buildings lowers the effectiveness of natural ventilation. In the form of suspended small particles, air pollutant lingers in these urban areas due to the lack of natural ventilation and form a problematic phenomenon called haze-fog (HF) (Zhang et al., 2015). People living in the extreme HF conditions suffer from long-term exposure to these small particles, which can penetrate deep into respiratory systems (Keshavarzian et al., 2012), and result in serious cardiovascular diseases (Brook et al., 2004). The risk of HF to urban residents, like any other toxicity, depends on the concentration and time of air pollutant's exposure ($C \times t$) (Blocken et al., 2020).

Air pollutant residual time of HF is defined as the exposure time that the premixed air pollutant suspended in an urban environment with initial concentration C_0 is washed away by wind flow. Although this transient phenomenon has been simulated recently in some studies by computational fluid dynamics (CFD) (Zhang et al., 2021, Zhang et al., 2015), there has been no physical study of air pollutant residual time of HF. This is largely due to the challenges with tracer gas techniques and the transient setup for simulating the premixed air pollutant. These techniques are widely used in wind tunnel experiments to measure mean concentration along with a continuous point discharge (Tominaga and Stathopoulos, 2013), in which supplies and exhaust are clear. However, to the best of our knowledge, no wind tunnel experiments have been conducted to measure the change of instantaneous concentration in a setup of premixed stagnant volume as HF.

In this study, detailed wind tunnel experiments were performed on air pollutant residual time around a generic cubical building in order to physically confirm the effect of wind-structure interaction on the air pollutant residual time and compile a validation database for CFD methods.

2. Outline of wind tunnel experiment

The experiments were carried out in the Boundary Layer Wind Tunnel (BLWT) located at The University of Sydney. The test section's dimension in this wind tunnel is 20 m in length, 2 m in width and 2 m in height. It was preferable to conduct the experiment in a smaller test section due to the challenges related to maintaining a uniform controllable distribution of tracer gas and its cost. Hence, a small test section with a fake ceiling and side walls was fabricated and placed on the wind tunnel's turntable. The wind tunnel was already calibrated to provide certain wind profiles corresponding to each terrain category using different combinations of vortex generators, barrier, and roughness elements. However, the wind profile needed to be adjusted inside the new test section.

2.1. Test Section and controlling doors

The test section is 4.2 m long, 0.8 m high, and 0.8 m wide, as shown in Figure 1 (a). A trap compartment with 1 m length is separated by two trap doors from the test section to trap the tracer gas inside. The distance between the trap compartment and the test section entrance was long enough to let the boundary layer developed before reaching the trap compartment. The trap doors were designed to move vertically and simultaneously upwards with a pulley and rope lifting design, as shown in Figure 1(b).

Wind flow needs time to be stabilized and reach a desirable wind speed in the wind tunnel prior to opening the trap compartment, which deteriorates the boundary layer developed in the test section by the trap doors. Therefore, another set of doors, called auxiliary doors here, is designed and installed at the test section entrance to stop the upcoming wind flow before the trap doors are lifted. These doors are fitted on a sliding frame next to the test section entrance and are designed to be opened sideways simultaneously using springs and rollers, as shown in Figure 1(b). This mechanism directs the approaching wind flow with the least vertical disturbance when it enters the test section. The steps for simulating the premixed air pollutant in this setup was as follows:

- Run the wind tunnel fan and reaching a desirable wind speed.
- Fill the trap compartment with the tracer gas.
- Start the concentration measurements.
- Move up the trap doors and open the auxiliary doors in sequence.

2.2. Experimental Settings

To generate a stable desirable low wind speed inside the test section, different combinations of meshes at the inlet and outlet of the test sections were tested, and a set of fine and coarse meshes were implemented for the inlet and outlet, respectively, as shown in Figure 1(c). A cube with a height of 0.2 m was chosen as the building model in this study. Instantaneous wind speeds were measured to determine the mean wind speed and turbulence intensity profiles prior to the actual tests using a hot-wire anemometer installed at different heights in the empty test section where the building model was positioned. A low turbulent near-uniform flow was developed, as shown in Figure 2. The wind speed and turbulent intensity at the building model's height were $U_{ref} = 1.2\ m/s$ and $I_{ref} = 10\%$, respectively.

2.3. Concentration Measurements

Measuring gas concentration at high frequency, which was a crucial part in this study, is difficult. The currently available instrumentations which have typical response of up to 400 Hz are flame ionization detectors (FID) and photo ionization detectors (PID). To measure an accurate residual time, it is important to capture the low gas concentration in this experiment. The detection limit of PID is around 100 ppb (parts per billion) which is much lower than FIDs with 1 ppm (parts per million) minimum detection.

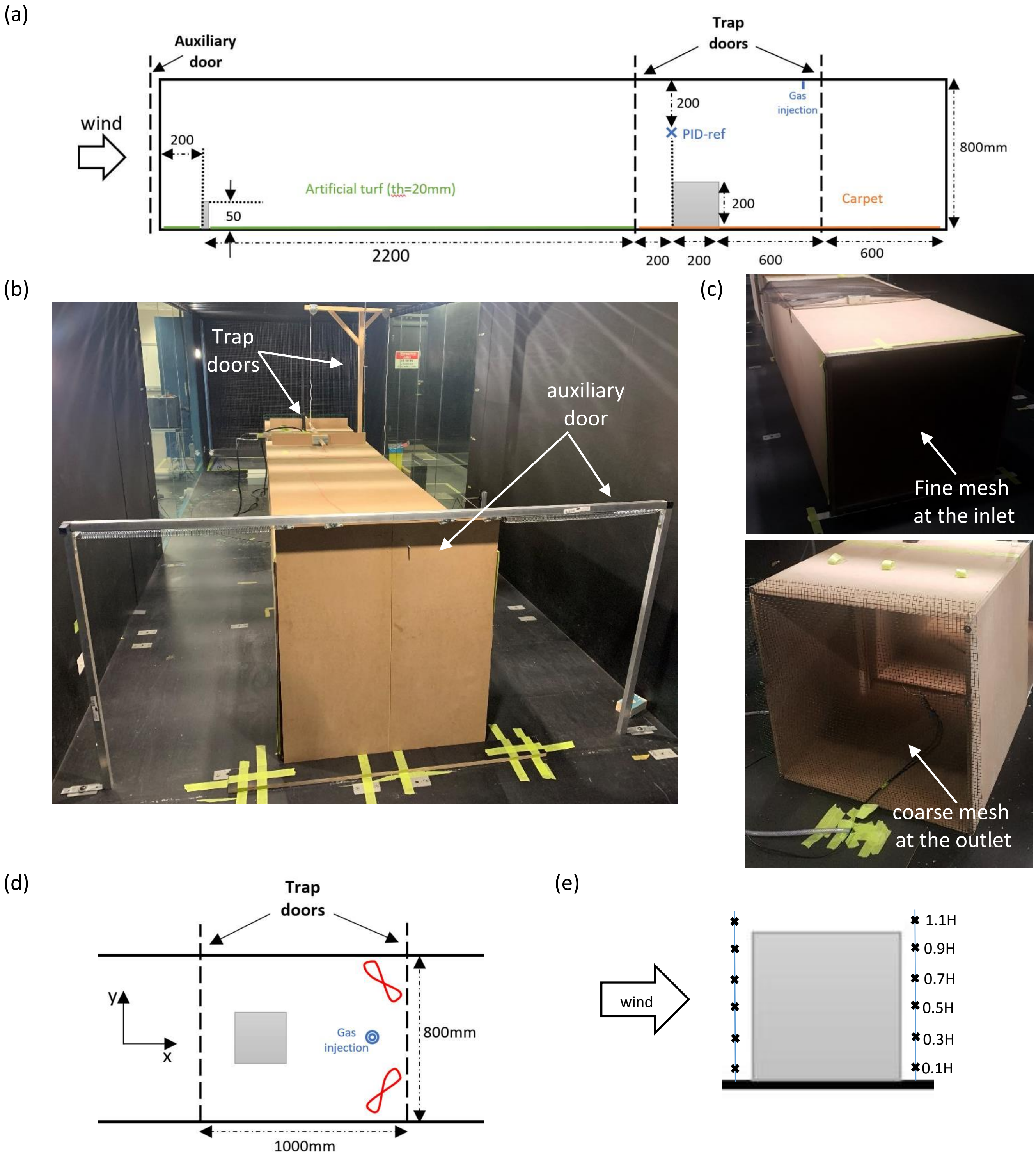

Figure 1. Experimental setup in wind tunnel: (a) Schematic side view, (b) trap doors and auxiliary doors, (c) meshed used for controlling wind speed, (d) schematic top view of trap compartment with the miniature fans, and (e) measurement points.

The mini-PID used in the experiment is designed to minimize flow disturbances. The sensor head dimension is 25.4 mm × 51 mm × 76 mm, which is much less bulky than the other available PIDs and FIDs. Two mini-PIDs were used in the test setup, a stationary PID which was positioned *400 mm* upper the building model aligned with the windward face, while a second PID was used to measure gas concentration around the building model. In order to further alleviate the flow disturbance inside the test section, the inlet needle of the PIDs was modified and placed further away from the sensor head using *300 mm* flexible tubing. Although adding the flexible tube causes a slight reduction in the frequency response of PID, the final tube length was chosen as a trade-off between blockage effects and the sensitivity of the sensor (Talluru et al., 2017).

The trap compartment was not airtight deliberately as the tracer gas mixture coming from a pressurized cylinder could build up excessive pressure prior to lifting the trap doors. The trap compartment was filled with a mixture of tracer gas with an initial concentration of *15000 ppm* isobutylene via a discharge tube positioned on the center of the test section's ceiling on the downstream end, as shown in Figure 1(a). The tracer gas diluted to *500 ppm* as the full-scale measuring range of PID to capture the immediate concentration decrease after the wind flow enters the trap compartment.

Two miniature fans installed at the two downwind corners of the trap compartment's ceiling to disperse the tracer gas releasing from the discharge tube uniformly in the relatively big volume of the trap compartment ($1 \times 0.8 \times 0.8\ m^3$), as shown in Figure 1(d). These small fans were in action when the trap compartment was being filled by the tracer gas before the trap doors lifted, and they did not disturb the wind flow inside the test section. Figure 1(e) displays the measurement positions on two lines in the vertical center plane with a distance of H/10 from the windward and leeward faces of the building model.

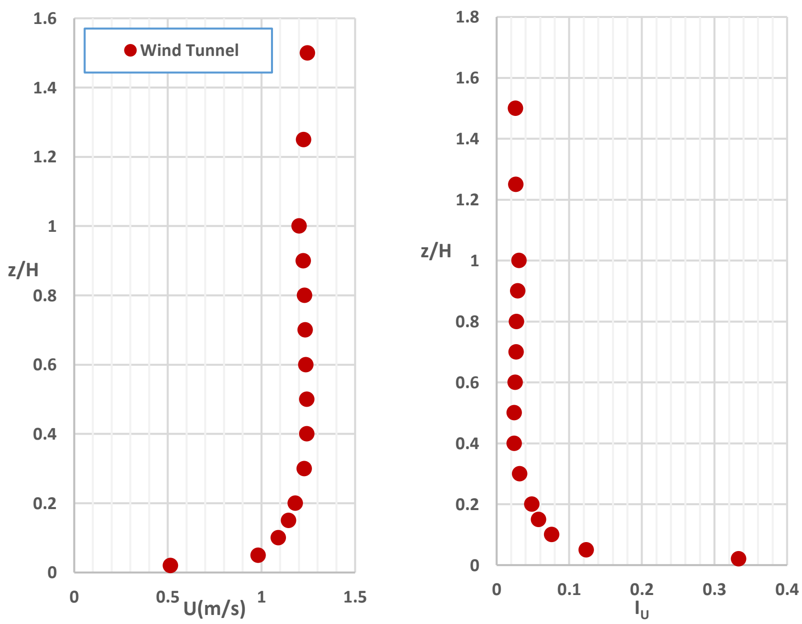

Figure 2. Wind speed and turbulent intensity measured in the empty test section.

3. Air pollutant residual time

In all measurements, the time-varying voltage signals from two PIDs mounted in the test setup translated into concentration (ppm) based on the calibration, which was conducted in situ before and after each experiment. An in-house manual setup, consisting of a gas-mixing chamber and two mass flow controllers, was used as the calibrator in experiments. As an example, Figure 3(a) shows translated concentrations of the measuring PID (PID-1) and the reference PID (PID-2). However, measured concentrations in this study were normalized by initial detected concentration for each PID ($C^* = C/C_0$) in order to calculate air pollutant residual time as a fall-time between the maximum and minimum concentrations as the main concern regardless of real concentration values. The air pollutant residual time was extracted from the transient jagging collected data as a fall time between 90% of the upper reference and 10% of the lower reference, as shown in Figure 3(b). For each measurement, the experiment was repeated three times to decrease the repeatability errors in the transient data collection.

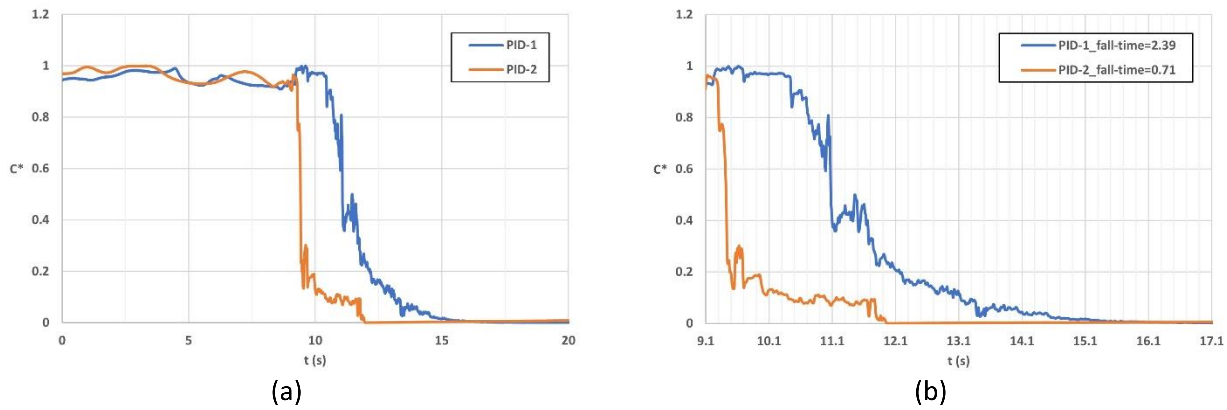

Figure 3. Concentration measurements of measuring PID (PID-1) and the reference PID (PID-2).

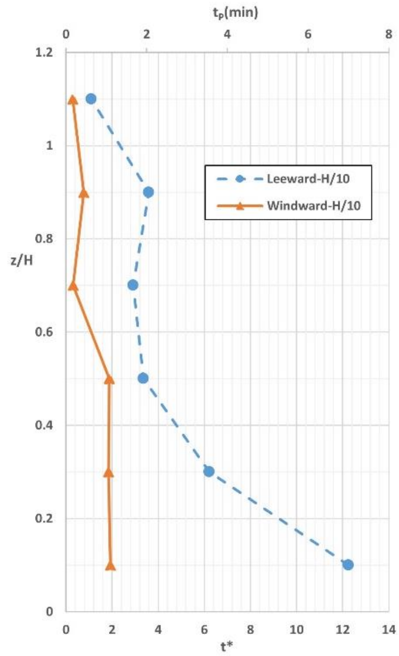

Figure 4. Vertical profiles of normalized and full-scale air pollutant residual time

In practice, the measured air pollutant residual time around the building model at the wind tunnel can show the air pollutant residual time for a full-scale prototype based on length scale and velocity scale. To do so, local air pollutant residual time is normalized (t^*) using the reference residual time. t^* is defined based on the fall-time extracted from the measured data of the measuring PID (t) and the reference PID (t_{ref}). Figure 4 shows the normalized air pollutant residual time $t^* = t/t_{ref}$ and the air pollutant residual time for the prototype for two vertical lines at a distance of H/10 from the building model's windward and leeward faces. Evidently, the HF air pollutant is diluted much faster at the windward region compared to the lee side of the building. This is largely due to the turbulent mixing and recirculation within the near at the lee side of the building, which keep the diluted HF air pollutant entrapped within the recirculation zone for a sustained period. The HF exposure time is longer for the points nearer to the ground, which suggests the air pollutant recirculates from higher to lower heights before eventually migrated upward and dispersed. The windward region's residual time shows that the HF air pollutant is removed quickly from the heights higher than the stagnation point on the windward face due to the upward dispersion. Due to the downwash effect, the HF air pollutant migrated downward and registered higher t^* values for the heights lower than the stagnation point.

Assuming the normalized residual time is equal for the scaled model and full-scale prototype ($t_m^* = t_p^* = t^*$), the prototype's residual time, $t_p = t^* t_{ref,p}$, is calculated by an estimation of the reference prototype residual time $t_{ref,p}$ for the length scale ($n = L_P/L_m$) and velocity scale as follows:

$$t_{ref,p} = t_{ref,m} \times n \times \frac{V_{ref,m}}{V_{ref,p}} \quad (1)$$

Typically, the wind tunnel scale model is between 1:100 and 1:400. Assuming the length scale for the building model in this study is 1:150 (H=30 m) and the velocity scale $\frac{V_{ref,m}}{V_{ref,p}} = 1$, Figure 4 shows the air pollutant residual time for the prototype (t_p) is in this study. For instance, the air pollutant residual time 3 m above the ground in the full scale (*H/10*) is more than 7 minutes for an isolated building, which can be quite a long time for certain air pollutant types with certain concentrations.

4. Conclusions

This paper presents a detailed wind tunnel setup and the subsequent experimental data of air pollutant residual time for haze-fog phenomenon around a generic isolated building. Normalized air pollutant residual time for the windward and leeward regions near the building model registered significantly different values. The residual time for the nearest measurement point to the ground was more than six times compared to the corresponding point in the windward region, indicating the suspended air pollutant was lingered and trapped in the lee side much more than the windward region. The results confirmed the effect of wind-structure interaction on air pollutant residual time which is challenging to obtain as a transient parameter in a wind tunnel study. Also, this study provides an experimental database for CFD validation studies in more complex cases.

References

BLOCKEN, B., VAN DRUENEN, T., VAN HOOFF, T., VERSTAPPEN, P. A., MARCHAL, T. & MARR, L. C. 2020. Can indoor sports centers be allowed to re-open during the COVID-19 pandemic based on a certificate of equivalence? *Building and Environment,* 180**,** 107022.

BROOK, R. D., FRANKLIN, B., CASCIO, W., HONG, Y., HOWARD, G., LIPSETT, M., LUEPKER, R., MITTLEMAN, M., SAMET, J. & SMITH, S. C. 2004. Air pollution and cardiovascular disease: a statement for healthcare professionals from the Expert Panel on Population and Prevention Science of the American Heart Association. *Circulation,* 109**,** 2655-2671.

KESHAVARZIAN, E., GHALATI, P. F., ABOUALI, O., AHMADI, G. & BAGHERI, M. H. Micro/Nano-Particle Deposition in the Airway of a 6-Year-Old Child From Nostril to the Third Generation. ASME 2012 Fluids Engineering Division Summer Meeting collocated with the ASME 2012 Heat Transfer Summer Conference and the ASME 2012 10th International Conference on Nanochannels, Microchannels, and Minichannels, 2012. 831-837.

TALLURU, K., HERNANDEZ-SILVA, C., PHILIP, J. & CHAUHAN, K. 2017. Measurements of scalar released from point sources in a turbulent boundary layer. *Measurement Science and Technology,* 28**,** 055801.

TOMINAGA, Y. & STATHOPOULOS, T. 2013. CFD simulation of near-field pollutant dispersion in the urban environment: A review of current modeling techniques. *Atmospheric Environment,* 79**,** 716-730.

ZHANG, Y., KWOK, K. C. S., LIU, X. P. & NIU, J. L. 2015. Characteristics of air pollutant dispersion around a high-rise building. *Environmental Pollution,* 204**,** 280-288.

ZHANG, Y., YU, Y., KWOK, K. C. S. & YAN, F. 2021. CFD-based analysis of urban haze-fog dispersion—A preliminary study. *Building Simulation,* 14**,** 365-375.